Formation process of interfaces and microdefects in nanostructured Ag studied by positron lifetime spectroscopy

1998 J. Phys.: Condens. Matter 10 3075

(http://iopscience.iop.org/0953-8984/10/13/023)

J. Phys.: Condens. Matter **10** (1998) 3075–3088. Printed in the UK PII: S0953-8984(98)86609-5

Formation process of interfaces and microdefects in nanostructured Ag studied by positron lifetime spectroscopy

X Y Qin†, J S Zhu‡, L D Zhang† and X Y Zhou§‖

† Institute of Solid State Physics, Academia Sinica, 230031 Hefei, People's Republic of China
‡ Structure Research Laboratory, University of Science and Technology, 230027 Hefei, People's Republic of China
§ Department of Modern Physics, University of Science and Technology of China, 230027 Hefei, People's Republic of China
‖ International Centre for Materials Physics, Academia Sinica, 110015 Shenyang, People's Republic of China

Received 4 August 1997, in final form 21 November 1997

Abstract. Nanostructured Ag (polycrystalline Ag with nanometre-sized grains), synthesized by inert-gas condensation plus *in situ* vacuum compaction, has been investigated by positron lifetime spectroscopy (PLS). The results indicate that there is a common character, i.e. only three lifetime components (τ_1, τ_2 and τ_3) are resolvable from the lifetime spectrum on each of the specimens synthesized under the whole compacting pressure range investigated (from 0.15 to 1.50 GPa). Corresponding to the three lifetime components, there are three types of defect (traps) in nanostructured Ag: (a) vacancy-like (VL) defects, (b) vacancy-cluster (VC) defects and (c) larger voids. Compacting pressure and annealing treatment has great influences on the positron annihilating behaviour. The lifetimes τ_1, τ_2 and corresponding intensities I_1, I_2 decreased irreversibly with compacting pressure and annealing temperature, indicating that the VL defects and VC defects are both mechanically and thermally unstable, and so it is inappropriate to consider them as structural elements in nanostructured Ag. Moreover, the interfaces in n-Ag can be considered as superpositions of VL defects on the normal ordered boundaries, and since the number and size of the VL defects change with external conditions, the interfaces in n-Ag can stay in various metastable states, which implies that its interfacial structures may range from total random states (gaslike) to complete ordered structures, depending on the number and size of the VL defects contained. The forming process of bulk nanostructured Ag revealed by PLS can be roughly divided into three stages: (1) formation stage of interfaces (compacting pressure $p \leqslant 0.6$ GPa); (2) rapid elimination of the three types of defect (0.6 GPa $< p <$ 1.1 GPa); (3) gradual elimination of those defects ($p >$ 1.1 GPa). Based on these results obtained on nanostructured Ag, a density criterion $D_c \approx 96\%$ that of the polycrystalline counterpart is proposed for the formation of bulk nanostructured materials.

1. Introduction

Recently there has been much interest in studying nanostructured materials [1] (n-materials) because these materials have shown many novel properties, such as high ductility in ceramics [2, 3], fast-diffusion behaviour in metals [4], high ion conductivity in ion conductors [5] and non-metallic electrical conductance in normal alloy [6]. Structurally, these novel properties are related to their large volume fraction of interfacial component (the interfacial volume fraction comprises about 50% in an n-material of a mean grain size 5 nm) and

0953-8984/98/133075+14$19.50

characteristics of their microdefects [1]. Clearly, the investigations of their interfacial phase and microdefects are of great importance to understanding their novel properties.

On the other hand, the understanding and clarification of the interfacial structures is of great fundamental significance, for so far different interfacial structure models in n-materials have been proposed. Gleiter *et al* [7] proposed that the grain boundaries in n-materials are of gaslike structures which have neither long- nor short-range order. This viewpoint seemed to have been supported by the experimental results of x-ray diffraction (XRD) [8], Mössbauer spectroscopy [9, 10], extended x-ray absorption fine structure (EXAFS) [11] and high-resolution electron microscopy (HREM) observations [12] etc. In contrast to the gaslike model, however, Siegel *et al* [13] and Thomas *et al* [14] considered that, based on their HREM observations on n-Pd and n-TiO_2, respectively, the interfacial structures in n-materials are similar to those in conventional polycrystalline materials (p-material), i.e. the interfaces in n-materials are of ordered structures. More recently, Li *et al* [15] observed that random and ordered interfacial structures co-exist in n-Pd by using HREM. Hence, the interfacial structures of n-materials remain an issue which has not been solved at present.

Positron lifetime spectroscopy (PLS) is particularly well suited for studying defects in solids [16], such as vacancies, vacancy clusters, voids and grain boundaries. Schaefer *et al* [17, 18] have investigated nanostructured Fe and Pd [19] by PLS and found four lifetime components which they attributed to positron annihilation at different types of defect, and they proposed that these defects can be considered as structural elements in n-materials [19]. Nevertheless, the forming process of interfaces and the changing behaviour of microdefects in n-materials during consolidation and anneal have not yet been investigated systematically at present. In addition, whether the proposed viewpoint of structural elements is appropriate or not remains to be approached.

One way to study the interfaces in n-materials is to monitor the forming process of the interfaces and the changing behaviour of the microdefects during this process in n-materials. As we will see, investigations on the process of interface formation by PLS will be expected to yield structural information of the interfaces as well as interfacial defects in n-materials, which is not only beneficial to understanding the characteristics of interfacial structures and microdefects, but also of instructive significance to synthesis of the n-materials.

In the present work, nanostructured Ag (n-Ag) is investigated by PLS. Part of the results have been communicated recently [20]. Here we lay a special emphasis on the effects of both compaction and anneal treatment on the behaviour of positron annihilation. Based on the results obtained by using PLS investigation on n-Ag, the forming process of interfaces, and the characteristics of interfacial structures and the microdefects of n-materials, are discussed.

2. Experimental methods

2.1. Synthesis of the specimens

The specimens of n-Ag were prepared by inert gas condensation followed by *in situ* vacuum compaction with the same principle as described in [7]. The raw material was 99.999% pure Ag powder. The vacuum chamber was firstly evacuated to a vacuum of 10^{-7} Pa, and then it was filled with He gas (4 N pure) to the pressure of $\sim$0.3 kPa. The nano-particles were obtained by evaporating the raw material through a tungsten boat, and collected on a cold finger filled with liquid nitrogen. After evaporation, the nano-powder was conveyed into a piston–anvil compacting unit and compacted *in situ* at ambient temperature for 2 minutes in a vacuum of 10^{-4} Pa. The uniaxial compacting pressure, p, was calculated from the applied

force divided by the cross-sectional area of the piston (6 mm in diameter) and ranged from 0.15 to 1.80 GPa. The obtained specimens were of disc shape, 6 mm in diameter and 0.1–0.5 mm in thickness. The mean grain sizes of the specimens were measured by using x-ray diffraction, with approximation-method analysis on the (111) reflection peak of n-Ag, on a Philip-PW1700 type x-ray diffractometer. The specimen densities were measured, based on Archimedes' principle, within an accuracy of $\pm 1\%$. As a reference, two conventional polycrystalline Ag (p-Ag) sheets were annealed sufficiently for measurements of the positron lifetime spectrum.

To investigate the effects of annealing treatment on positron lifetime spectra, four groups of specimens (two specimens to a group) compacted under 1.3 GPa were scanning annealed, at the rate of 40 K min^{-1} to desired temperatures in argon atmosphere and then cooled at the rate of 320 K min^{-1} to room temperature for measurements of positron lifetime spectra.

2.2. Positron lifetime measurements

Positron lifetime experiments were performed by using a standard fast–fast coincidence ORTEC system with a time resolution of 290 ps (FWHM). As a positron source, ^{22}NaCl of about 10 μCi was sealed in thin Kapton ($\approx$1.3 mg cm^{-1}). Two identical sample pieces were sandwiched together with the positron source. The measured lifetime spectra were analysed using the PATFIT-88 program taking into account the annihilation in the source. In order to obtain a good statistical accuracy, each spectrum always contained at least 1×10^6 counts, and the measurement was repeated twice.

3. Results and discussion

Figure 1 shows the typical positron lifetime spectra of n-Ag specimens (mean grain size 31 nm) compacted under various pressures, and that of p-Ag. It can be roughly seen that as compacting pressure, p, increased, the intensity of long-lifetime component decreased (see figure 1). A multicomponent analysis of the lifetime spectrum on the p-Ag specimens shows that only a single lifetime $t = 138 \pm 2$ ps was obtained, which coincides well with the literature value (138 ps) [21]. However, from the lifetime spectra of n-Ag specimens compacted under various pressures a common character was revealed—that there are three lifetime components in each of the spectra: a short lifetime τ_1 (164–203 ps) with an intensity of 50–56%; an intermediate lifetime τ_2 (380–400 ps), with an intensity of 42–46%; as well as a long lifetime τ_3 (1200–1700 ps). The concrete values of the lifetimes and the corresponding intensities depend on the applied compacting pressure.

For the n-Ag specimens which were scanning annealed to different temperatures, the same character as that of as-prepared (as-p) n-Ag specimens was obtained, i.e. only three lifetime components were resolvable from each spectrum whose concrete lifetimes and intensities depend on the annealing temperatures. In the following sections, first we will discuss briefly the three lifetime components (section 3.1), and then discuss the influences of compacting pressure (section 3.2) and anneal treatment (section 3.3) on the behaviour of positron annihilation. Finally, the characteristics of interfacial structures and microdefects, as well as the formation criterion of bulk n-materials, will be discussed (section 3.4).

3.1. Three lifetime components

As an example, table 1 lists the analytical results of the positron lifetime spectrum on the n-Ag specimen compacted under 1.0 GPa. It can be seen from table 1 that each lifetime

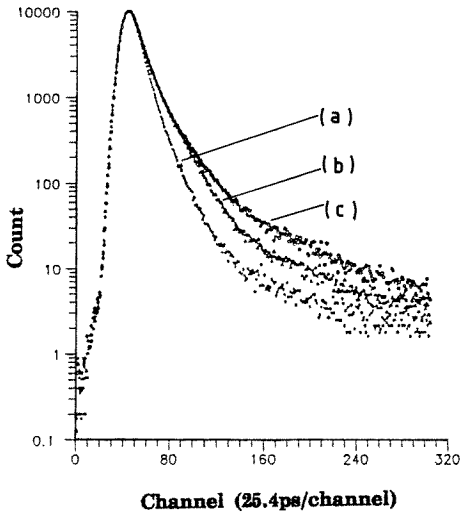

Figure 1. Positron lifetime spectra on (a) polycrystalline Ag and on n-Ag specimens compacted under (b) 1.5 GPa, (c) 0.6 GPa. The counts at peaks of all the curves have been normalized to 10 000.

Table 1. Positron lifetimes and intensities of corresponding components measured on a nanostructured Ag specimen compacted under the pressure 1.0 GPa.

Lifetime (ps)			Intensity (%)		
τ_1	τ_2	τ_3	I_1	I_2	I_3
173 ± 4	445 ± 12	1608 ± 24	59.3 ± 1.8	39.1 ± 1.6	1.6 ± 0.6

of the three components is substantially longer than that of the positrons annihilated in the delocalized free state ($\tau_f = 138$ ps) in bulk p-Ag. This result indicates that almost all the positrons injected into the specimen were localized before annihilation. On the other hand, since the mean grain size of the as-prepared n-Ag specimens (31 nm) is much smaller than the diffusion length of positrons in single-crystal Ag ($L_+ = 110$ nm) [22], the thermalized positrons could easily diffuse into the interfaces. Recent HREM observations [12, 15] revealed that in n-metals the crystallite lattice is fairly perfect; intragranular defects, such as lattice dislocations and lattice vacancies, were only detected occasionally. In contrast, a great number of interfacial defects, such as nanovoids, random (or extended) boundaries were detected [12, 15]. Clearly, these defects can act as positron traps. Hence, it can be concluded that near-saturation trapping and annihilation of the positrons occurred at interfacial traps of the n-Ag specimens.

The short lifetime $\tau_1 = 173 \pm 4$ ps (see table 1) is greater than the bulk lifetime in p-Ag ($\tau_1 = 138$ ps) and smaller than the lifetime trapped at the monovacancies ($\tau_{1v} = 206$ ps) [21] in p-Ag. This component with lifetime τ_1 has two physical origins: free annihilation within the grains and annihilation at interfacial traps. Since the mean grain size of n-Ag (30 nm) is smaller than the positron diffusion length in bulk silver (900 nm), a dominant fraction of the annihilations takes place at the interfacial traps. If one assumes that the trapping is in fact saturated (all annihilations take place at traps), one can attribute the short lifetime to the positrons annihilating at the open-volume interfacial defects, whose size is of

the order of that of a monovacancy. These free volumes associated with τ_1 are one type of interfacial defect, which is called here vacancy-like (VL) defect for convenience, although the mean size of these defects may vary with compacting pressures (see below).

The intermediate lifetime $\tau_2 = 445 \pm 12$ ps with comparable intensity to that of τ_1 could be attributed to positrons trapped at the free volumes at the intersections of two or three crystallites (triple junctions) whose volumes are equivalent to about 10–15 vacancies estimated by the lifetime τ_2. In fact, nanovoids with the size 3–5 nm at the triple junctions have been observed in n-Pd [15] synthesized with the same method as that used here. This type of defect is called here vacancy-cluster (VC) defects for the sake of convenience.

Similar to the case in n-Fe [18], the long lifetime $\tau_3 = 1608 \pm 24$ ps with an intensity of about 2% could result from the annihilation of *ortho*-positronium (*o*-Ps) formed at the internal surfaces of larger voids (or porosity) in n-Ag. Evidence of the existence of these larger voids is the occurrence of some bubbles, with diameters of several microns to dozens of microns, on the surface of n-Ag specimens during annealing, which could be caused by expansion of the gases within the large voids [23]. In n-Fe [18], however, not only τ_3 (1200 ps) but also τ_4 (4000 ps) was detected, with a total intensity between 10% and 30% which is much greater than the intensity (2%) of τ_3 observed here. This difference could also be explained by the density difference between n-Fe [18] and n-Ag specimens. Clearly, smaller specimen density indicates that there were many more free volumes with a mean size much larger in n-Fe [18] than in n-Ag used here, which results in formations of more *o*-Ps in n-Fe specimens, with a longer lifetimes because of the reduction of the collision rate of the Ps with void walls [24]. These larger voids are the third type of defect in n-Ag specimens.

3.2. The influence of compacting pressure on the behaviour of positron annihilation

Figure 2 shows the mean position lifetime $\overline{\tau}$ as a function of compacting pressure p. It can be seen that the mean lifetime $\overline{\tau}$ decreases monotonically from 350 to 300 ps with increase of pressure p. This result agrees with the quasi-hydrostatic pressure experiments [25]. Since the values of τ_1, τ_2 and τ_3 are related to the mean volume sizes of the three types of defect, the value of $\overline{\tau}$, to some extent, represents the amount of total free volumes of the defects in an n-Ag specimen. Hence, the decrease of $\overline{\tau}$ with pressure p indicated that the total free volumes reduce with increase of compacting pressure, resulting in densification in n-Ag specimens. This conclusion, in fact, coincides well with the results of density measurements (figure 3). It can be seen that the density of n-Ag rose rapidly from 94% to about 96% as compacting pressure increased from 0.15 to 0.60 GPa and then it reached nearly 99% that of conventional p-Ag as p increased further to 1.80 GPa.

Positron lifetimes (τ_1, τ_2 and τ_3) and corresponding intensities (I_1, I_2 and I_3) of the three components are shown, as a function of compacting pressure, in figures 4 and 5 respectively. It can be seen that the lifetime τ_1 decreased monotonically from 203 ± 9 to 164 ± 3 ps as the pressure p increased from 0.15 to 1.50 GPa (figure 4(a)), indicating that the mean volume of the VL defects associated with τ_1 shrank with increasing compacting pressure. This result shows directly a high compressibility of these interfacial VL defects.

The intermediate lifetime τ_2, on the other hand, shows different behaviour from that of τ_1 with compacting pressure (figure 4(b)). It increased first from 382 ± 12 to 450 ± 20 ps when pressure p increased from 0.15 GPa to 0.60 GPa, and then decreased to 402 ± 7 ps as p increased further to 1.5 GPa, leaving a maximum around 0.6 GPa. The rapid decrease of τ_2 with pressure at $p > 1.00$ GPa would originate from shrinkage of VC defects caused by compactness, while the initial increase of τ_2 reflects the increase of the mean volume of the

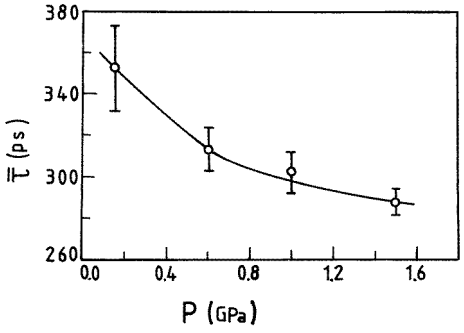

Figure 2. Variation in mean positron lifetime with compacting pressure.

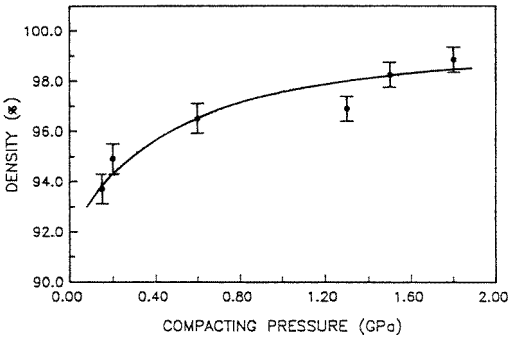

Figure 3. The variation in density (relative to conventional polycrystalline Ag) of n-Ag specimens with compacting pressure.

VC defects. We may assume that under lower pressures ($p < 0.6$ GPa), the main effect of compactness would be formation of interfaces accompanied by and/or realized through the transformations of VC defects into VL defects. The assumption of VC defects transforming to VL defects in the pressures $p < 0.6$ GPa was supported by the change in behaviour of I_2 with pressure p (see figure 5(a)). It can be seen from figure 5(a) that, in the pressure range from 0.15 to 0.6 GPa, the intensity I_2 decreased rapidly from 46% to 29%, accompanied by rapid increase of intensity I_1 from 49% to 65%. In addition, it is conceivable that smaller VC defects are easier than larger ones to transform into VL defects. As a result, smaller VC defects are first to be transformed into VL defects, leading to a greater proportion of larger VC defects than in the case of applying lower pressures among the residual VC defects. Hence, the mean size of the residual VC defects becomes greater, being manifested by the increase of τ_2 with p.

The formation of interfaces could also be detected from the rapid increase of intensity ratio I_1/I_2 in the pressures $p < 0.6$ GPa (figure 5(c)). According to the trapping model, positron annihilation intensity I_i in type i of traps [18]:

$$I_i = s_i C_i/(1/\tau_0 - 1/\tau_i) \tag{1}$$

where C_i denotes the concentrations of various types, i, of trap; s_i denotes the corresponding specific trapping rates and τ_0 is the residence time of positrons in the delocalized lattice state. Therefore, the ratio I_1/I_2 is related to concentrations of the two types of trap by the

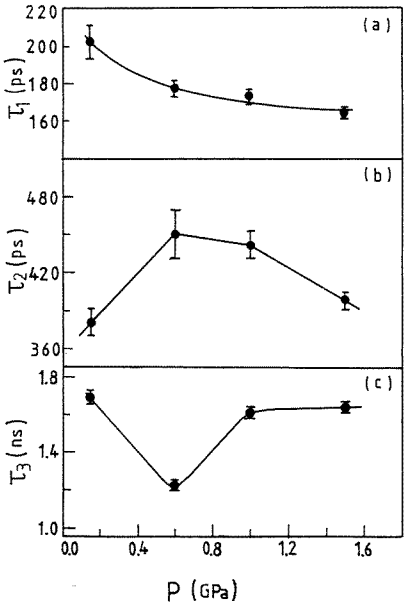

Figure 4. Plots of the three positron lifetimes against compacting pressure: (a) short lifetime τ_1; (b) intermediate lifetime τ_2; (c) long lifetime τ_3.

formula:

$$I_1/I_2 \approx s_1C_1/s_2C_2. \tag{2}$$

Assuming equal trapping rates per unit area for interfaces with VL defects and VC defect–crystallite interfaces, then the ratio I_1/I_2 reflects the area ratio of the two types of defect. Hence, the rapid increase of I_1/I_2 with p under pressures below 0.6 GPa (figure 5(c)) indicates the rapid increase of interfacial area with respect to that characterized by τ_2, exhibiting the formation process of the interfaces of n-Ag.

The relation between interface formation and transformation of VC defects to VL defects could be understood in terms of the vacancy diffusion mechanism model (see schematic drawing, figure 6). As three crystallites are brought into contact with one another (in the case of two dimensions), a VC defect–triple junction void forms (see figure 6(a)). At this time as an external pressure is applied, the total diffusion current $\boldsymbol{J}$ has the form [26, 27]:

$$\boldsymbol{J} = -D\left(\nabla C + \frac{C}{KT}\frac{2\gamma}{r^2}\boldsymbol{r} + \frac{C}{KT}\nabla\phi\right) \equiv \boldsymbol{j}_d + \boldsymbol{j}_s + \boldsymbol{j}_p. \tag{3}$$

Here, $\boldsymbol{j}_d = -D\nabla C$, $\boldsymbol{j}_s = -(DC/kT)2\gamma\boldsymbol{r}/r^2$ and $\boldsymbol{j}_p = -(DC/kT)\nabla\phi$ are concentration gradient, surface stress of defects and other stress potential gradient (compacting pressure, for instance) induced diffusion currents, respectively (where D denotes self-diffusion coefficient, C and ∇C denote vacancy concentration and its gradient, γ and r denote surface energy and radius of curvature of VC defects, ϕ denotes stress potential, T is temperature and k is the Boltzmann constant). It should first be pointed out that, at ambient temperatures, diffusion occurs mainly through interfaces [28] and the vacancy diffusions caused by $\boldsymbol{j}_d$, $\boldsymbol{j}_s$ and $\boldsymbol{j}_p$ are from VC defects to interfaces. The latter conclusions can be expounded briefly here. (1) The vacancy concentration in interfaces is lower than that in VC defects (which can be considered as a combination of several vacancies), so $\boldsymbol{j}_d$

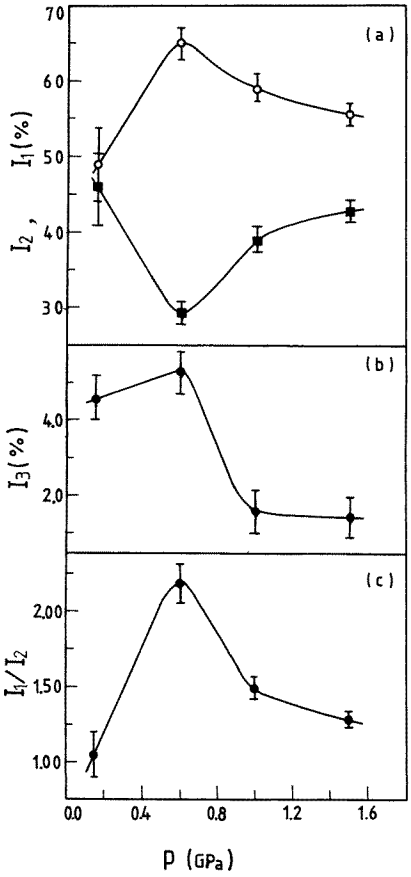

Figure 5. The intensities of the three components as a function of compacting pressure: (a) intensity I_1 (○), I_2 (■); (b) intensity I_3 and (c) intensity ratio of short- to intermediate-lifetime components I_1/I_2.

caused by ∇C is from VC defects to interfaces; (2) since the surface stress $-2\gamma/r$ tends to reduce size of the VC defects, the direction of $\boldsymbol{j}_s$ is also from VC defects to interfaces; (3) when a compressive stress is applied (as shown in figure 6(a)), the contact spots (neck) of the crystallites between them are compressed, so vacancies are inclined to diffuse from the VC defect to the joining spots (interfaces) to relax the stress. Accompanying the vacancy transport from the VC defects to the formed interfaces (or the atom transport from the interfaces to the VC defects), the VC defects shrink and interface area increases (as shown schematically in figure 6(b)). Since at ambient temperature the atomic relaxation and vacancy diffusion from interfaces to crystallites is slow, the transported free volumes in newly formed interfaces are 'frozen in' and could act as positron traps responsible for component t_1. To compare roughly the contribution of compacting pressure with that of surface stress to the current $\boldsymbol{J}$, substituting γ of silver [29] with 1.3 J m^{-2} as well as $|\nabla\phi|$ ($\approx p$) with 1.0 GPa in j_s and j_p, we obtained $j_p/j_s \approx 1$ for a VC defects with a diameter of 4 nm [15], indicating that both contributions are of same order. Obviously, for larger VC defects (with greater r), the effect of applied pressure become relatively more important. Moreover, in the case of larger VC defects, the actual area sustaining the applied force (i.e.

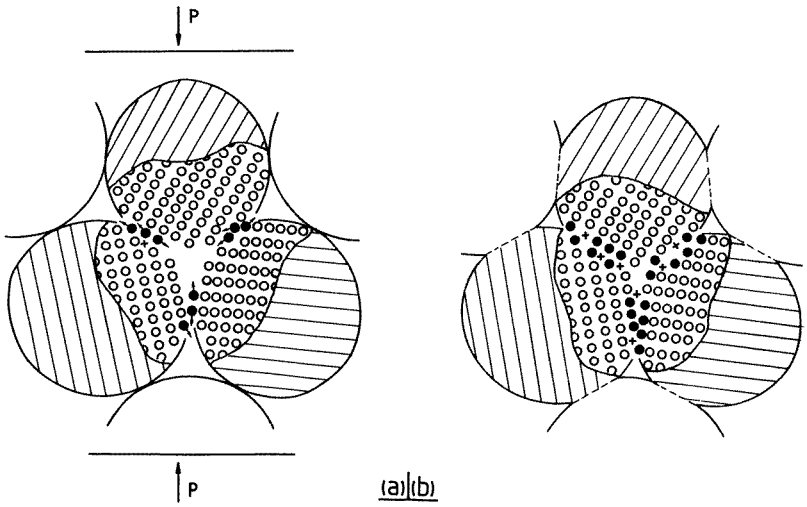

Figure 6. Schematic drawing (in two-dimensional case) of the relation between transformation of VC defects into VL defects and the forming process of interfaces under the action of compacting pressure: (a) the initial stage of interface formation (solid circles denote interfacial atoms); (b) under the action of applied compressive stress, accompanying diffusion of atoms the VC defects shrink and VL defects develop (marked by + in the figure), leading to increase of interfacial area.

having formed interfaces) is much smaller than the cross-sectional area of the piston from which p was calculated. So the actual stresses $|\nabla\phi|$ at the interfaces are much greater than external pressure p. Hence, at the initial stage of the formation of interfaces, the dominant driving force is the compacting pressure.

When compacting pressure increased further, however, the main effects of the compactness could be: (i) rapid transformation of the larger voids into VC defects; (ii) the shrinkage of the VC defects and elimination of VL defects. These conclusions are based on the following facts:

We can see from figure 5(b) that in the pressure range from 0.6 to 1.0 GPa, I_3 decreased rapidly from about 5.4% to 1.5%, accompanied by the increase of I_2 from 29% to 39% (figure 5(a)), implying the transformation of larger voids to VC defects. This transformation could occur through collapse of the larger voids caused by compacting pressure as shown schematically in figure 7, where four VC defects form after collapse of one larger void. The intensity I_1 decreased monotonically with increasing pressure ($p > 0.60$ GPa) (figure 5(a)), showing the elimination of the VL defects at the interfaces of n-Ag. The elimination of VL defects can also be detected from the decrease of τ_1 with pressure p (figure 4(a)) and the shrinkage of VC defects can be detected from decrease of τ_2 with pressure at $p > 0.6$ GPa (figure 4(b)).

The change of τ_3 with pressure p appears irregular (figure 4(c)). This is because the lifetime of Ps is not only related to void size but also sensitive to contamination of void surfaces [30].

The interpretation of positron annihilation behaviour with compacting pressure above agrees with the result of microhardness measurements. Figure 8 gives the Vickers microhardness of n-Ag as a function of compacting pressure (experimental details were given in [23]). It can be seen that the hardness of n-Ag increases rapidly from 0.62 GPa to

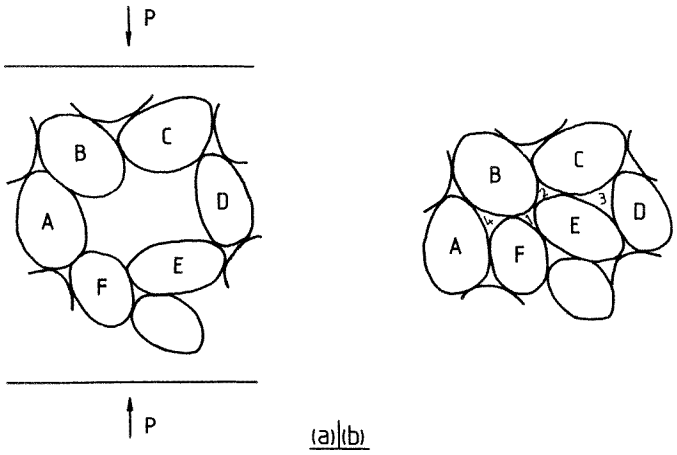

Figure 7. Schematic drawing (in two-dimensional case) of the transformation of large voids to VC defects under the action of compacting pressure: (a) a large void in n-Ag which is constituted by the six crystallites labelled A–F; (b) under the action of compacting pressure, four VC defects (labelled 1–4) form at the expense of elimination (collapse) of the large void.

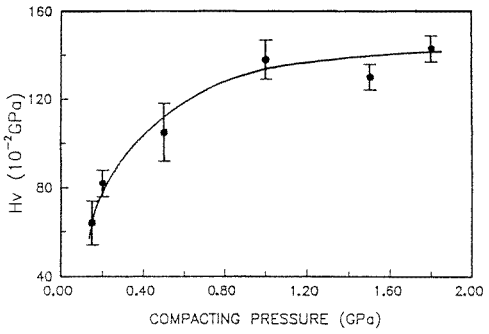

Figure 8. The variation in Vickers microhardness of the n-Ag specimens with compacting pressure.

about 1.2 GPa as pressure p rises from 0.15 to 0.6 GPa, and then the hardness increases slowly as p increases further. Since grain boundaries (interfaces) act as strong obstacles to dislocation movements [31] and so possess strong resistance to plastic deformation, the rapid increase of interfaces (boundaries) in the pressure range 0.15 GPa $< p <$ 0.60 GPa inevitably leads to the rapid enhancement of the strength of n-Ag. The slow increase of hardness with p as $p >$ 1.0 GPa could reasonably be explained by the gradual elimination of interfacial VL defects as well as both gradual shrinkage of VC defects and reduction of large voids in n-Ag.

3.3. The effects of anneal treatment on the behaviour of positron annihilation

Four groups (two specimens to a group) of n-Ag specimens compacted under the pressure 1.3 GPa were scanning annealed, at 40 K min^{-1}, separately to 510, 650, 870 and 990 K. Positron lifetime spectra were measured at ambient temperature for these specimens.

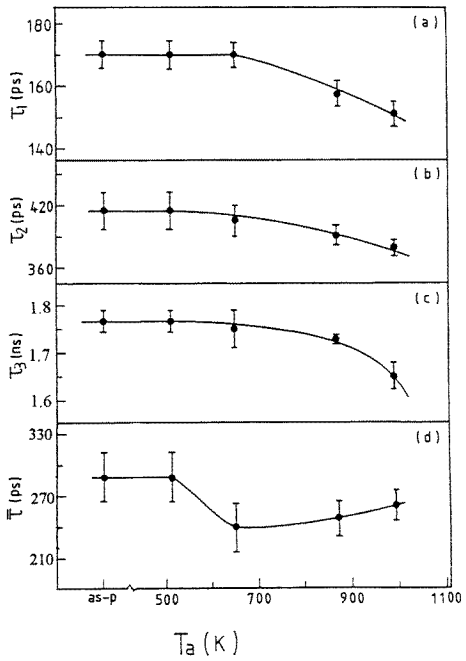

Figure 9. The plots of the three positron lifetimes as well as mean lifetime on the specimens compacted at 1.3 GPa against uplimit temperature, T_a, of scanning anneal at the rate 40 K min^{-1}: (a) lifetime τ_1; (b) lifetime τ_2; (c) lifetime τ_3; (d) mean lifetime $\overline{\tau}$.

Figure 9 shows the positron lifetimes as a function of uplimit temperature, T_a, of scanning anneal. It can be seen that the lifetimes τ_1, τ_2 and τ_3 begin to decrease as the anneal temperatures $T_a > 510$ K. As T_a increases further, their decreases become faster (see figure 9). These results indicate that the main effect of anneal treatment is to cause shrinkage of all the three types of defect, which was confirmed by the change in behaviour of $\overline{\tau}$ (figure 9(d)). Here, it is worthwhile to note that the resistances of the three types of defect to heating, or their thermal stability, are not different from one another substantially, which implies that the mechanisms controlling the elimination process of the three types of defect in this temperature range have no notable difference.

The influence of annealing on the intensities of the three lifetime components is shown in figure 10. It can be seen that (figure 10(a)) as $T_a < 650$ K, I_1 and I_2 did not change obviously; as $T_a > 650$ K, the intensity I_1 decreased rapidly. In contrast with I_1, the intensity I_2 rose promptly as $T_a > 650$ K. Because of the changes of both I_1 and I_2, the intensity ratio I_1/I_2 decreased abruptly as $T_a > 650$ K (figure 10(b)), which, as discussed in section 3.2, indicates that the concentration of VC defects increased with respect to that of VL defects. A similar result was also reported in n-Pd [19], and can be interpreted as the agglomeration of vacancy-type defects to microvoids. In addition, it is worthwhile to note that in the temperature range from 510 to 650 K I_1 and I_2 did not change obviously, while I_3 decreased rapidly. This phenomenon would reflect desorption of the adsorbed gases within porosity. The increases of I_3 with T_a as $T_a > 650$ K would then reflect the bubbling effect during annealing at higher temperatures in the n-Ag specimens, as observed by some of the present authors with scanning electron microscopy [23].

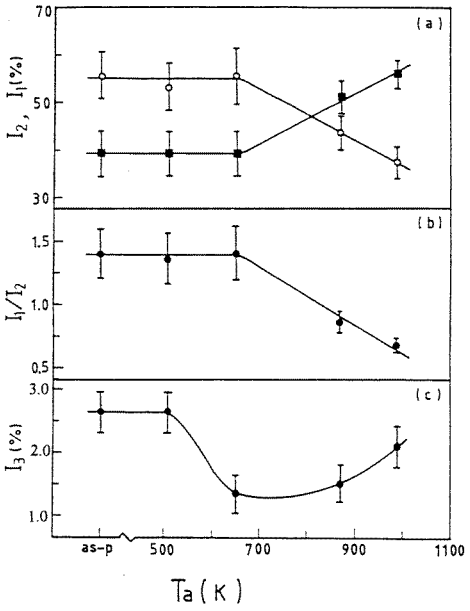

Figure 10. The intensities of the three components as a function of uplimit temperature, T_a, of scanning anneal (at 40 K min^{-1}): (a) intensity I_1 (○), I_2 (■); (b) intensity ratio I_1/I_2; (c) intensity I_3.

3.4. The characteristics of interfaces and microdefects, and the formation criterion of bulk nanostructured materials

3.4.1. The characteristics of interfaces and microdefects. As discussed in section 3.1, corresponding to the three lifetime components, there are three types of defect in n-Ag. Among them, the third type—large voids—could be considered as macroscopic defects, based on their large sizes. Hence, we discuss mainly the other two types of defect here. Since the positron lifetimes (τ_1, τ_2 and τ_3) represent a mass centre of a certain lifetime distribution [18], the free volume estimated by τ_1 is only a mean value, and does not represent a definite single size. In addition, the investigations of PLS in the compacting process indicate that the size of VL defects in n-Ag changes with compacting pressure (figure 4(a)). In other words, the VL (or VC) defects can possess various sizes, depending on synthetic conditions and history (such as compacting pressure, annealing temperature etc). Moreover, since the VL defects reside in interfaces of n-materials, the interfaces in n-materials can be considered as a superposition of VL defects on normal ordered boundaries. Hence, the order of the interfaces in n-materials depends on the numbers and sizes of the VL defects present. Because the number and size of the VL defects can be altered by external conditions (compacting pressure, for instance), generally the interfaces of n-materials can stay in various metastable states, ranging from total random (gaslike) structures (containing sufficient VL defects) to complete ordered structures (containing nearly no VL defects). Therefore, the proposed gaslike model [7] and ordered model [13, 14] of interfacial structures of n-materials only reflected its two extreme cases. The present viewpoint on the interfacial structure coincides with the HREM observations [15], where both random and ordered boundaries were found to coexist in n-Pd.

As mentioned above, the number and size of the VL defects decreased irreversibly with compacting pressure (figures 4(a), 5(a)), which means that this kind of defect is mechanically unstable. Moreover, annealing experiments indicate the volumes of VL defects shrink on heating (figure 9(a)), which agrees with the HREM observations in n-Pd [15], where transformations of random boundaries to ordered ones, under electron beam irradiation *in situ*, were noticed. These results indicate that the VL defects are not only mechanically unstable, but also thermally unstable. Therefore, it is inappropriate to consider this type of defect as structural elements in n-Ag. Likewise, the PLS investigations indicate that the VC defects can be transformed irreversibly to VL defects under the action of compacting pressure (figures 4(b), 5(a)) and shrunken under the effect of annealing (figure 9(b)). Hence, it is also inappropriate to consider them as a structural element in n-Ag.

3.4.2. The criterion of forming bulk nanostructured materials. As discussed in section 3.2, under the pressures $p < 0.6$ GPa, the main effect of compactness is to form interfaces of n-Ag, and as $p > 0.6$ GPa, its main effect is to eliminate various types of defect, leading to the ordering of the interfaces. In other words, the formation of interfaces in n-Ag is complete essentially under the pressure $p \approx 0.6$ GPa. Hence, based on present results of PLS investigations, a criterion of forming 'bulk' n-Ag could be proposed: to form a bulk n-Ag, a minimum compacting pressure $P_c = 0.6$ GPa is needed.

Since the degree of the formation of interfaces and/or the content of free volumes in an n-material not only depend on the values of compacting pressure but also are related to other factors, such as the duration of the applied pressure, the temperature during compaction and the ductility and the strength of the material itself, the compacting pressure is not a optimal index. In contrast, the densification of an n-material is a better comprehensive index of the formation of interfaces. Hence, for more universality the criterion may be expressed in the form of density. Corresponding to the pressure $P_c = 0.6$ GPa, a density $D_c \approx 96\%$ is derived from figure 3. Therefore, to form a 'bulk' n-material, a density $D \geqslant 96\%$ that of the polycrystalline counterpart is needed. The criterion $D_c \approx 96\%$ agrees with the empirical standard in ceramics [32], where a material with a density of 90%–95% is usually considered as 'dense material'.

4. Summary and conclusions

Studies of positron lifetime spectroscopy have been performed and the following conclusions can be drawn.

(1) Corresponding to three positron lifetime components τ_1, τ_2 and τ_3, there are three types of defect in n-Ag, which include vacancy-like (VL) defects, vacancy-cluster (VC) defects and large voids. The fact that the free volumes and concentrations of the two types of microdefect reduce irreversibly during compaction and anneal treatment indicates that they are both mechanically and thermally unstable, and therefore it is inappropriate to consider them as structural elements in n-Ag.

(2) The interfaces of n-Ag can be considered as superposition of VL defects on the normal ordered boundaries. Since the number and size of the VL defects change with external conditions, the interfaces in n-Ag can stay in various metastable states, which implies that they may range from total random states (gaslike) to a complete ordered structure, depending on the number and size of the VL defects contained.

(3) The formation process of bulk n-Ag can be divided into three stages: (i) formation stage of interfaces ($p < 0.6$ GPa); (ii) rapid elimination stage of the three types of defect

(0.6 GPa $< p <$ 1.1 GPa) and (iii) gradual elimination stage of the three types of defect ($p >$ 1.1 GPa). Based on the results obtained on n-Ag by PLS, a criterion of the formation of bulk n-materials can be proposed: a minimum density $D_c \approx 96\%$ that of the polycrystalline counterpart is needed.

References

[1] Gleiter H 1989 *Prog. Mater. Sci.* **33** 223
[2] Karch J, Birringer R and Gleiter H 1987 *Nature* **330** 536
[3] Birringer R 1989 *Mater. Sci. Eng.* A **117** 33
[4] Mutschele T and Kirchkeim R 1987 *Scr. Metall.* **21** 135
[5] Wu X J, Su F, Qin X Y, Xie B and Ji X L 1993 *Mater. Res. Symp. Proc.* vol 286 (Amsterdam: Elsevier) p 27
[6] Qin X Y, Zhang L D, Wu B M, Tian M L, Du Y L, Yang D S and Cao L Z 1996 *J. Appl. Phys.* **80** 4776
[7] Birringer R, Herr U and Gleiter H 1986 *Trans. Japan Inst. Met. Suppl.* **27** 43
[8] Zhu X, Birringer R, Herr U and Gleiter H 1987 *Phys. Rev.* B **35** 9085
[9] Birringer R, Gleiter H, Klein H P and Marguardt P 1984 *Phys. Lett.* **102A** 365
[10] Herr U, Jing J, Birringer R, Gonser V and Gleiter H 1987 *Appl. Phys. Lett.* **54** 472
[11] Haubold T, Birringer R, Lengeler B and Gleiter H 1989 *Phys. Lett.* **135** 461
[12] Wunderlich W, Ishida Y and Maurer R 1990 *Scr. Metall.* **24** 403
[13] Thomas G J, Siegel R W and Eastman J A 1990 *Scr. Metall.* **24** 201
[14] Parker J C and Siegel R W 1990 *Appl. Phys. Lett.* **57** 943
[15] Li D X, Ping D H, Ye H Q, Qin X Y and Wu X J 1993 *Mater. Lett.* **18** 29
[16] Schaefer H E, Gugelmeier R, Schmolz M and Seeger A 1984 *Microstructural Characterization of Materials by Non-microscopical Techniques* ed N Hessel Andersen *et al* (Roskilde: Risø National Laboratory) p 489
[17] Schaefer H E and Wurschum R 1987 *Phys. Lett.* **119A** 370
[18] Schaefer H E, Wurschum R, Birringer R and Gleiter H 1988 *Phys. Rev.* B **38** 9545
[19] Schaefer H E, Eckert W, Stritzke O, Wurschum R and Templ W 1989 *Positron Annihilation* ed L Dorikens-Vanpraet, M Dorkens and D Segers (Singapore: World Scientific) p 79
[20] Qin X Y, Zhu J S, Zhou X Y and Wu X J 1994 *Phys. Lett.* **193A** 335
[21] Mackenzie I K 1983 *Positron Solid State Physics* ed W Brandt and A Dupasquier (Amsterdam: North-Holland) p 196
[22] Soininen E, Huomo H, Huttunen P A, Mukinen J, Vehanen A and Hantojavi P 1990 *Phys. Rev.* B **41** 6227
[23] Qin X Y, Wu X J and Zhang L D 1995 *Nanostruct. Mater.* **5** 101
[24] West R N, Alam A, Walters P A and McGervey J D 1982 *Positron Annihilation* ed P G Coleman, S C Sharma and L M Diana (Amsterdam: North-Holland) p 337
[25] Wurschum R, Greiner W and Schaefer H E 1993 *Nanostruct. Mater.* **2** 55
[26] Haasen P 1986 *Physical Metallurgy* 2nd edn (Cambridge: Cambridge University Press) p 192
[27] Feng D and Qiu D R 1987 *Structures and Defects (Physics of Metals 1)* (Beijing: Academia Sinica Press) pp 525–6
[28] Ashby M F 1974 *Acta Metall.* **22** 275
[29] Feng D and Qiu D R 1987 *Structures and Defects (Physics of Metals 1)* (Beijing: Academia Sinica Press) pp 399
[30] Mogensen O E, Eldrup M, Mørup S, Ømbo J W and Topsøe H 1985 *Positron Annihilation* ed P C Jain, R M Singru and K P Gopinathon (Singapore: World Scientific) p 980
[31] Haasen P 1986 *Physical Metallurgy* 2nd edn (Cambridge: Cambridge University Press) p 287
[32] Burggraaf A J, Keizer K and Winnubst A J A 1991 *Ceramics Today—Tomorrow's Ceramics* ed P Vincenzini (Amsterdam: Elsevier) p 1311